ELSEVIER

Journal of Power Sources 111 (2002) 255–267

JOURNAL OF POWER SOURCES

www.elsevier.com/locate/jpowsour

Two- and three-electrode impedance spectroscopy of lithium-ion batteries

J.Y. Song, H.H. Lee, Y.Y. Wang, C.C. Wan*

Department of Chemical Engineering, National Tsing-Hua University, 300 Hsinchu, Taiwan

Received 12 March 2002; accepted 22 May 2002

Abstract

The interfacial impedance between PVDF/HFP-based electrolytes and lithium metal continues to increase and attains a delicate kinetic equilibrium upon prolonged storage. The graphite anode, on the other hand, is found to remain inert towards the electrolytes. Its interfacial impedance does not vary with increasing storage time or in the presence of different lithium salts. In addition, it is found that the impedance of a Li–C half-cell consists of the impedances of two interfaces and is therefore often mistakenly used in the interpretation of the behaviour of a single carbon electrode. Thus, a three-electrode impedance study is required. It is found that an inductive loop appears in the low-frequency region of the impedance spectrum of a carbon electrode immediately after the first lithium-intercalation step, which probably implies that an adsorption–desorption phenomenon might exist at the interface. Moreover, another inductive effect, which arises from the connecting leads, also appears in the high-frequency region. Finally, the cathode is found to be the major source of cell impedance and increases with increasing cycle number.

Keywords: Carbon electrode; Impedance; Lithium-ion battery; Storage time

1. Introduction

Recently, there has been intensive research on Li-ion batteries, especially with respect to the complex interfacial reactions between electrolytes and electrodes. Carbonaceous materials are the most widely used negative materials for Li-ion batteries because lithium can randomly and stably intercalate or de-intercalate into them. Many reports have discussed the mechanisms and interfacial reactions of lithium intercalation into carbon, especially for graphite, for the past 20 years. Impedance spectroscopy is one of the most promising tools for the modelling and diagnosis of interfacial reactions. It can even analyse the sources of battery impedance and identify battery failure by comparison with an appropriate equivalent-circuit model. Early researchers [1–3] proposed that impedance resulted from many factors, such as charge transfer, Li^+ diffusion in electrodes, passive film, etc. The shape and value of the resistance in the impedance spectrum were found to be strongly affected by solvents, particle sizes, thickness of electrodes, and stack pressure [4–6]. Without systematic and integrated comparison of these spectra, incorrect interpretations could arise. In this work, therefore, impedance studies have been performed with both two-electrode and three-electrode Li–C systems and then the variation of impedance during cycling has been analysed.

2. Experimental

The preparation of liquid electrolytes and polymer membrane electrolytes, together with cell assembly, were all conducted in an argon-filled glove box (Model MB 150-M, MBraun). The moisture content of the atmosphere in the box was controlled under 2 ppm. The graphite used in this study was a flaky SFG44 artificial graphite material (TIMCAL AG, Sins, Switzerland) with an average particle size of ~44 μm. The electrodes were prepared by first making a slurry of the graphite powder with 10 wt.% commercial PVDF/HFP copolymer (Kynar FLEX® 2801, Elf Atochem North America Inc.) dissolved in acetonitrile. The mixture was spread and dried at 80 °C for 10 min. The dried polymer–graphite composite sheet was pressed into a ~98 μm film and then cut into 1.2 μm diameter discs. A typical graphite electrode contains a loading of 9.5 mg cm^{-2}. The electrolytes were a composite of battery-grade chemicals

* Corresponding author. Tel.: +886-3-572-1664; fax: +886-3-571-5408.
E-mail address: ccwan@mx.nthu.edu.tw (C.C. Wan).

0378-7753/02/$ – see front matter
PII: S0378-7753(02)00310-5

which included lithium hexafluorophosphate ($LiPF_6$, Hashimoto), lithium perchlorate ($LiClO_4$, Tomiyama), ethylene carbonate (EC, Merck), γ-butyrolactone (BL, Merck), and commercial PVDF/HFP copolymer (Kynar FLEX® 2801, Elf Atochem North America Inc.). All these chemical materials were used as received without further purification. Lithium metal foil (FMC) was used for the counter and reference electrodes in two- or three-electrode impedance measurements. Commercial prismatic-type Li-ion cells with stacked electrodes (093488, SYNergy ScienTech Corp.) were also used for a comparative study. The major cathode and anode materials were $LiCoO_2$ and carbon, respectively.

An AUTOLAB frequency response analyser (Eco Chemie, Holland) was employed for obtaining complex impedance spectra in the frequency range 10 Hz to 50 kHz. In the two-electrode impedance measurement, coin cells were used as test cells. In the three-electrode impedance measurement, purpose-built test cells (3.5 mAh) and commercial 093488 prismatic Li-ion cells (1100 mAh) were employed. A schematic diagram that allows impedance measurements to be made in a three-electrode configurations is shown in Fig. 1. The sample was placed between two stainless-steel (SS 316) blocking electrodes with mirror-like surfaces in an O-ring sealed cell. A lithium metal foil, which acted as a reference electrode, was sandwiched between two electrolyte membranes to control the distance between the working and the reference electrodes to the thickness of an electrolyte membrane (∼80 μm). For the three-electrode configuration in commercial 093488 prismatic Li-ion cells, the procedure used in [7] was adopted. A conductive wire, on to which a tiny piece of lithium metal was attached, was inserted into the cell to serve as a reference electrode. After assembling, the reference electrode was in the middle of the electrode sheets.

3. Results and discussions

3.1. Two-electrode impedance studies

The Li-ion battery impedance comes from the electrolyte (including separator), the carbon anode, and the transition metal oxide cathode. In order to analyse the interfacial phenomenon of one electrode, either the $LiCoO_2$ cathode or the carbon anode, a cathode half-cell (Li–$LiCoO_2$) or an anode half-cell (Li–C) is usually used. A Li–C half-cell still, however, combines the interfacial properties of the C electrode and the Li metal electrode. Thus, its impedance spectrum does not exactly reflect the interfacial impedance of a single C electrode. This has commonly been overlooked in past research. To illustrate this point, a series of two-electrode impedance measurements has been conducted to observe interfacial changes in detail.

First, symmetric test cells with identical working and counter electrodes were used to investigate the properties of a single interface. The impedance spectra of a symmetric Li–Li test cell in 1 M $LiPF_6$ + EC/BL (1:1 v/v) upon prolonged storage is presented in Fig. 2(a). In this respect, it consists of two Li|electrolyte interfaces so that the interfacial resistances in Fig. 2(a) represent a doubling of a single Li electrode. The plot exhibits a large semicircle in the high-frequency region, followed a small semicircle in the

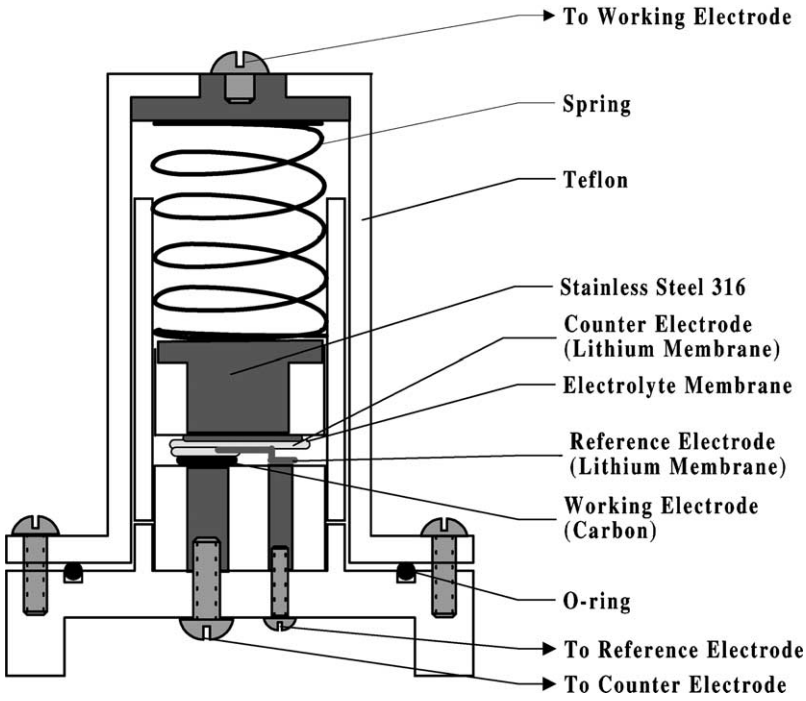

Fig. 1. Three-electrode test cell.

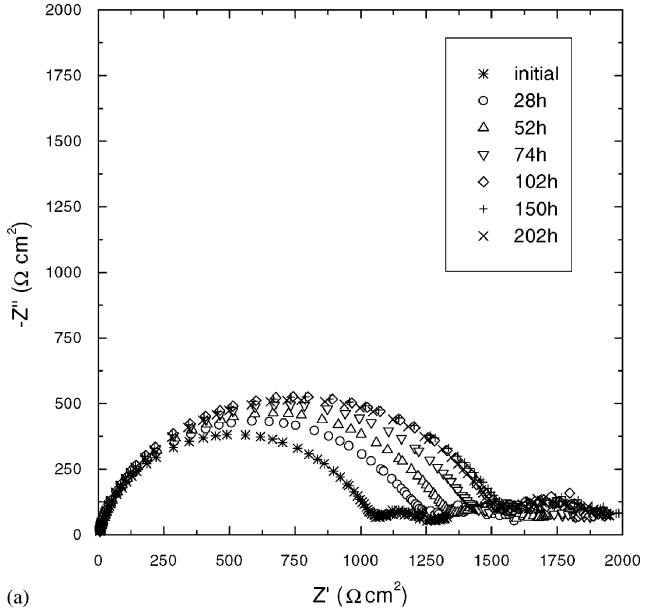

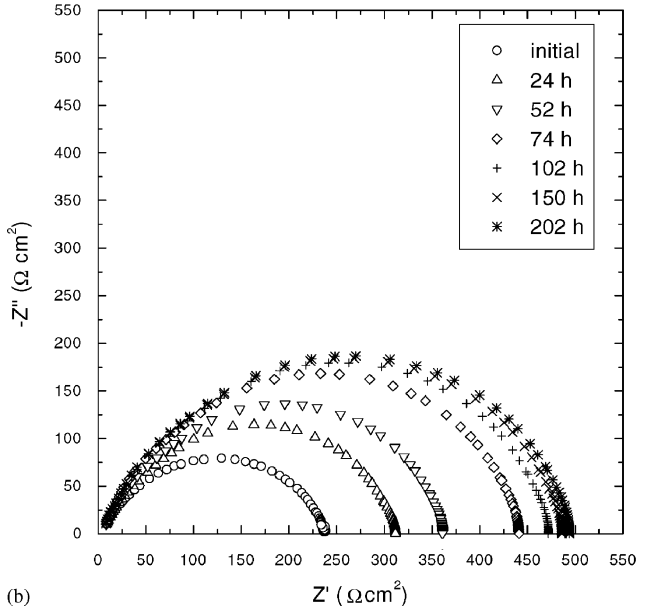

Fig. 2. Impedance spectra of symmetric Li–Li test cell in: (a) 1 M $LiPF_6$ + EC/BL (1:1 v/v); (b) 1 M $LiClO_4$ + EC/BL (1:1 v/v), prolonged storage.

low-frequency region. As described earlier [8,9], the high-frequency intercept at the Z'-axis corresponds to the electrolyte resistance, the left semicircle corresponds to the passivated film impedance on the lithium metal surface, and the right semicircle represents the charge transfer. Apparently, the right semicircle remains constant with increasing storage time, whereas the left one grows, although it gradually reaches a steady-state. This means that the interface between lithium metal and 1 M $LiPF_6$ + EC/BL attains the meta-stable situation upon prolonged storage so that this impedance does not increase further.

The impedance spectra for lithium metal and 1 M $LiClO_4$ + EC/BL, shown in Fig. 2(b), is obviously different from that in Fig. 2(a). There is only a large semicircle which corresponds to a passivated film impedance. Thus, the difference between Fig. 2(a) and (b) may be related to the passivated film produced from decomposition of different electrolytes. The decomposition of $LiPF_6$ produces protons which can enhance the conductivity and result in lowering of the impedance of the passivated film and charge transfer. Over the same frequency range, therefore, the passivated film impedance of $LiPF_6$ is lower than that of $LiClO_4$ electrolytes, so the charge-transfer impedance is barely noticeable in Fig. 2(b). To verify this reasoning, the ac voltage amplitude was raised to 50 mV for the $LiClO_4$ system, as shown in Fig. 3. The semicircle corresponding to charge transfer eventually appears in the low-frequency region. This proves the above hypothesis.

It is noteworthy that the impedance of the passivated film is strongly related to the initial state of the lithium metal. The lower the oxidation of the lithium surface at the beginning, the smaller is the passivated film impedance. So, a direct comparison of the magnitude of the impedance of $LiPF_6$ and $LiClO_4$ electrolytes in Fig. 2 is not meaningful since their initial oxidised states are not necessarily equal. Therefore, only the kinetic properties of interfacial passivated processes from spectra are observed, such as growing rate and stability, so that the phenomena of interfacial changes upon storage and cycling can be illustrated.

Similarly, a symmetric C–C test cell is used to observe the variation of the C|electrolyte interface upon prolonged storage, as shown in Fig. 4. The spectrum displays a line vertical to the Z'-axis which corresponds to the capacitive reactance instead of the diffusion effect. This is because there are no intercalated lithium atoms in the carbon matrix so the carbon matrix serves as the blocking electrode for lithium atoms. It can also be seen that the capacitive reactance remains constant with increasing time, which means the carbon electrode is inert toward $LiPF_6$ + EC/BL solution.

An enlargement of Fig. 4(a) in the high-frequency region is given in Fig. 4(b). The high-frequency intercept is about 4 $\Omega\,cm^2$, which corresponds to the electrolyte resistance. Comparing Fig. 4 with Fig. 2, these two intercepts are found to be consistent. Based on the conductivity of the electrolyte (1.45×10^{-3} S cm^{-1} at room temperature) and the distance between the two electrodes (5.6×10^{-3} cm), it is estimated that the uncompensated solution resistance is 3.86 $\Omega\,cm^2$, which matches the intercept closely. From these results in two-electrode tests, it can be concluded that the electrolyte resistance comes mainly from the ohmic resistance of the system, and thus it does not change with either the polarisation potential or the type of the electrodes.

To the right of the intercept is a clear semicircle, as shown in Fig. 4(b). This semicircle maintains its resistance at about 15 $\Omega\,cm^2$ (so a single C electrode is 7.5 $\Omega\,cm^2$), unlike the impedance of the passivated film, which increases upon

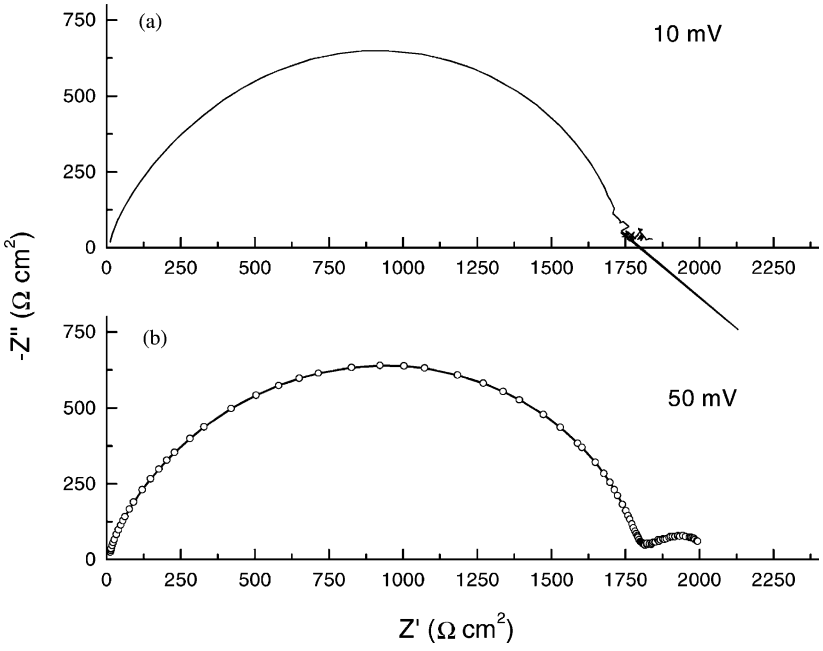

Fig. 3. Impedance spectra of symmetric Li–Li test cell in 1 M $LiClO_4$ + EC/BL (1:1 v/v). Applied ac voltage is (a) 10 mV, (b) 50 mV.

prolonged storage. Moreover, there are no intercalated lithium atoms in the carbon so that charge transfer and Li^+ diffusion do not occur. Hence, the semicircle should be due to the wetting of carbon. The impedance includes the intrinsic electronic resistance of the carbon electrode and the contact resistance of the carbon particles. Namely, there is no passivated film produced at the surface of graphite. The resistance only comes from the interior of the carbon electrode.

Similar properties exist in the $LiClO_4$ electrolyte system, as shown in Fig. 5. The shape and magnitude of the spectrum are similar to that in Fig. 4, which illustrates that graphite electrodes are inert towards these two-electrolyte systems.

With the impedance data of single carbon and lithium electrodes available as reference, it is possible to analyse the more complex impedance spectra of a Li–C test cell which contains the interface between the lithium metal and the carbon electrodes. So, the Li–C impedance spectra should be the sum of the spectra of the two electrodes. The three spectra are given in Fig. 6. The semicircle of a Li–C cell in Fig. 6 relates to the impedance of the carbon electrode and the passivated film on the lithium metal surface. The impedance of the later is much large than the former, so however, their spectra overlap and cannot be distinguished from each other clearly. Otherwise, the linear region of the Li–C cell at low frequency obviously involves only the capacitive effect of the carbon electrode.

After the statical impedance studies, the impedance spectra during the charge–discharge process were studied. The impedance spectra of the first discharge (the first intercalation of lithium atoms into carbon) at various open-circuit voltages (OCV) are presented in Fig. 7(a). A fresh Li–C cell displays obvious passivated film impedance (a large semicircle) at the lithium metal surface. When discharge current passes through the cell, however, the passivated film is damaged by oxidation of lithium metal so that its impedance immediately decreases. An enlargement of the spectra for 0−0.22 V discharge OCV is shown in Fig. 7(b). The spectra are similar in shape with two semicircles at the left hand followed by a 45° declining line. When comparing these with the spectrum of a fresh cell, the declining line at low frequency is greatly different from the steep one in the preceding case. Namely, the capacitive effect is substituted for the diffusion of lithium atoms in carbon (Warburg effect) after lithium intercalation into graphite. The Warburg effect enhances as the amount of intercalated lithium atoms increases. In addition, the second semicircle between the declining line and the high-frequency semicircle remains unchanged at about 40–90 Ω in spite of decreasing OCV, this is considered to be a charge-transfer impedance (R_{CT}). The left semicircle at high frequency in Fig. 7(b), which differs among various voltages, is evidently due to the passivated film impedance (R_{SEI}) of the two and C electrodes. As discharge proceeds, R_{CT} rarely changes but R_{SEI} slowly decreases. In other words, the passivated film has greater effect than charge transfer on the first discharge process. Nevertheless, there seems to be a mild increase of R_{SEI} below 0.094 V OCV, which may be related to the accumulation of solvated ion clusters on the passivated film.

During the charge process (Fig. 8), the passivated film on the carbon surface is destroyed by the de-intercalation of lithium ions from carbon so that R_{SEI} decreases very fast. The semicircle becomes more complex due to the overlap of the spectra for the charge transfer and the passivated film.

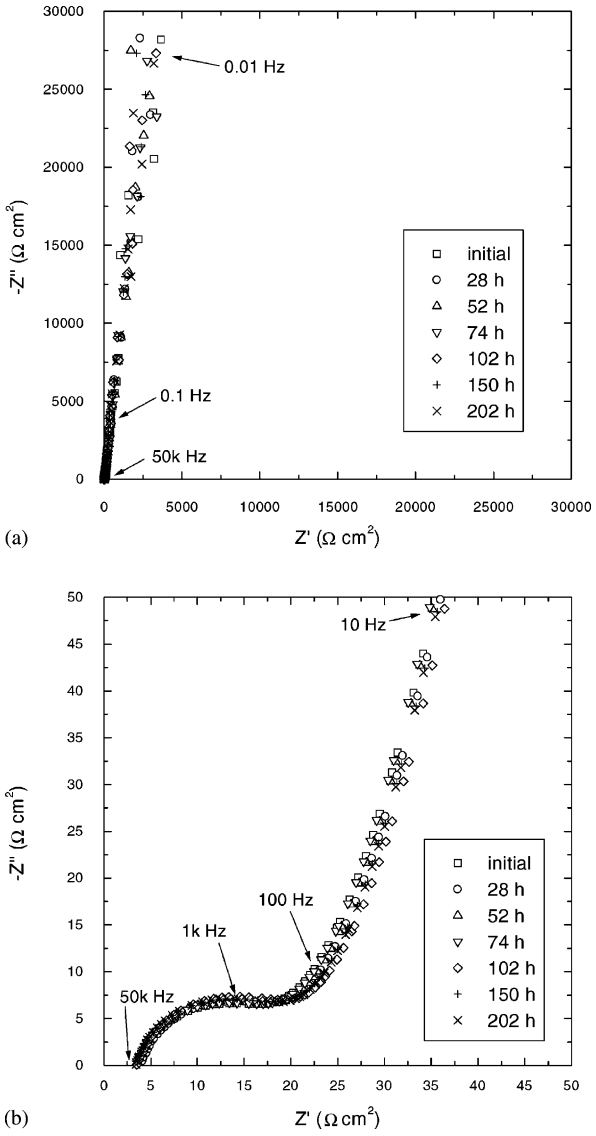

Fig. 4. Impedance spectra of symmetric C–C test cell in 1 M $LiPF_6$ + EC/BL (1:1 v/v) after prolonged storage. (a) Spectrum in total-frequency range. (b) Enlargement in high-frequency range.

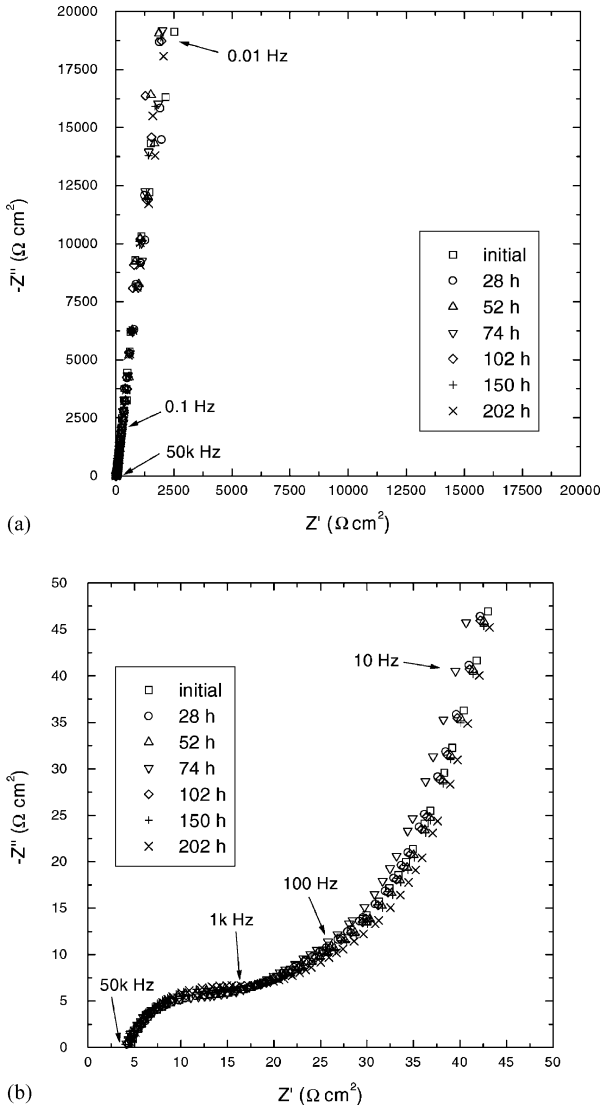

Fig. 5. Impedance spectra of symmetric C–C test cell in 1 M $LiClO_4$ + EC/BL (1:1 v/v) after prolonged storage. (a) Spectrum in total-frequency range. (b) Enlargement in high-frequency range.

The spectra are all similar below 0.5 V OCV. As the OCV exceeds 0.7 V, all lithium ions leave the carbon electrode, and the right side of these spectra becomes a nearly vertical line which corresponds to the capacitive effect from a fresh cell.

The results of impedance measurement for cycles following the first cycle are displayed in Fig. 9. The spectra were all measured at an OCV above 1.5 V, namely, all lithium ions were de-intercalated from carbon, so that they represent the capacitive effect of the fresh cell instead of the Wargurg impedance of discharged state at low frequency. The spectra in the high-frequency region are enlarged in Fig. 9(b) and (c). These semicircles related to the surface condition of lithium and carbon electrodes are smaller than that of a fresh cell, and become larger with increasing cycle number. Take the 10th cycle for example. If this cell is stored for 24 h after 10 cycles, the semicircle also enlarges. This phenomenon indirectly proves that the semicircle is induced from the intrinsic electronic resistance and contact resistance of the carbon electrode and the passivated film on the two electrodes rather than from the charge-transfer effect. The above discussions clarify how contributions from the interfacial factors can be studied based on impedance spectra of the Li–C half-cell alone.

3.2. Three-electrode impedance studies of Li/C half-cells

The two-electrode impedance studies have an obvious disadvantage in that it is difficult to distinguish the impedance of various anodes and cathodes from a combined spectra. To measure accurately how a single electrode changes with cycling tests, three-electrode impedance studies are necessary.

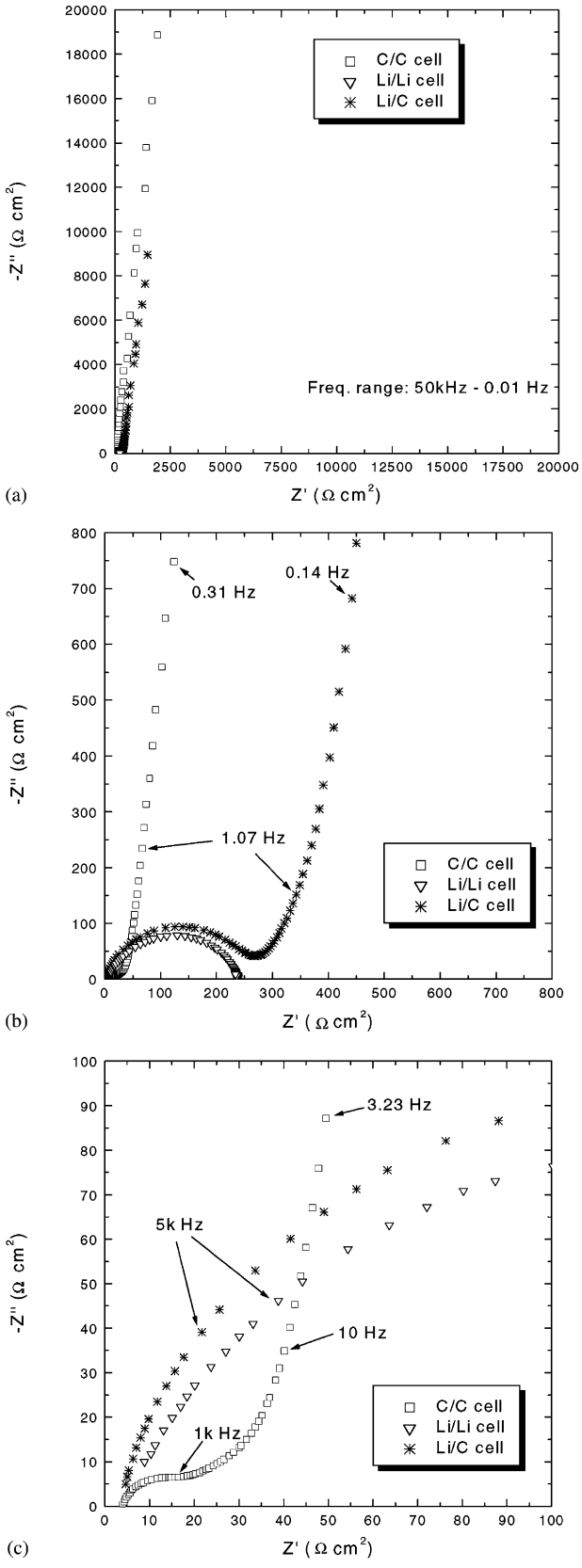

Fig. 6. Comparison of impedance spectra with Li–C half-cell, symmetric C–C and Li/Li test cells in 1 M $LiClO_4$ + EC/BL (1:1 v/v). (a) Spectrum in total-frequency range. (b) Enlargement in middle-high frequency range. (c) Enlargement in high-frequency range.

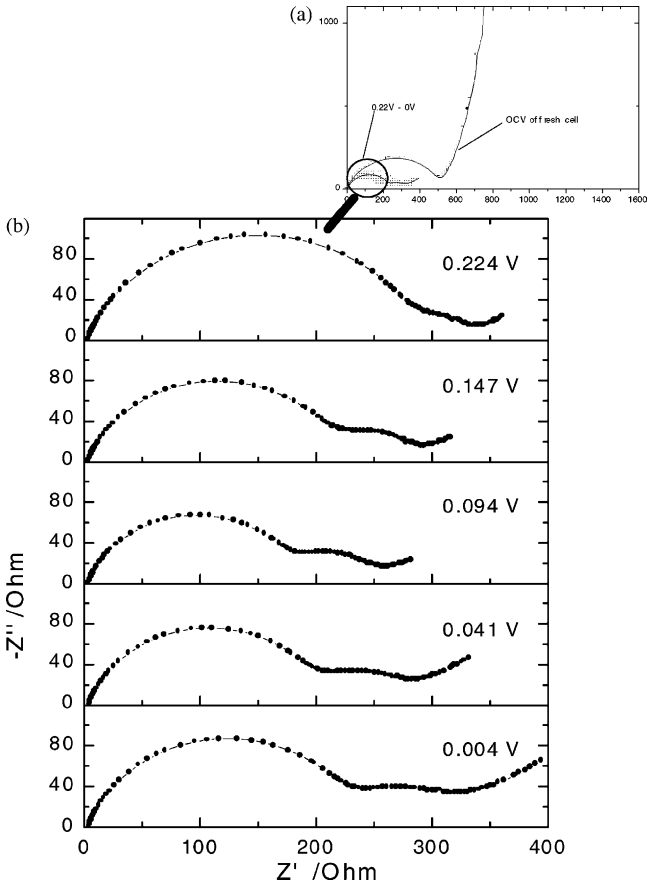

Fig. 7. (a) Variation of impedance spectra of Li–C half-cell in 1 M $LiPF_6$ + EC/BL (1:1 v/v) during first discharge (Li-intercalation) process. (b) Enlargement spectra for OCV 0.224–0 V discharge.

The impedance spectra of a specific Li–C half-cell measured in two-electrode and three-electrode configurations are shown in Fig. 10. As labelled in the figure, "full cell" indicates the two-electrode system and "graphite only" is the three-electrode system with a graphite working electrode. These two spectra both similarly show an intercept at high frequency ("full cell" is 7.7 Ω, and "graphite only" is 3.7 Ω) followed with a semicircle and a vertical line at low frequency. Generally speaking, the high-frequency intercept (R_{ex}) results from three sources: (i) the solution resistance between the working and reference electrodes (R_u); (ii) the wire resistance of the system (R_l); (iii) the interfacial contact resistance between electrode and electrolyte (R_s). For cells with small capacity or small electrode area, R_{ex} is usually larger than R_l and R_s. Under this condition, the high-frequency intercept directly corresponds to R_u. The R_u of the three-electrode system (3.7 Ω) is smaller than that of the two-electrode system (7.7 Ω) because the reference electrode is positioned as close to the working electrode as possible in the three-electrode system. Next, the middle-frequency semicircles of "full cell" and "graphite only" are due to the different sources. The semicircle of the "full cell" results from carbon and lithium metal electrodes as

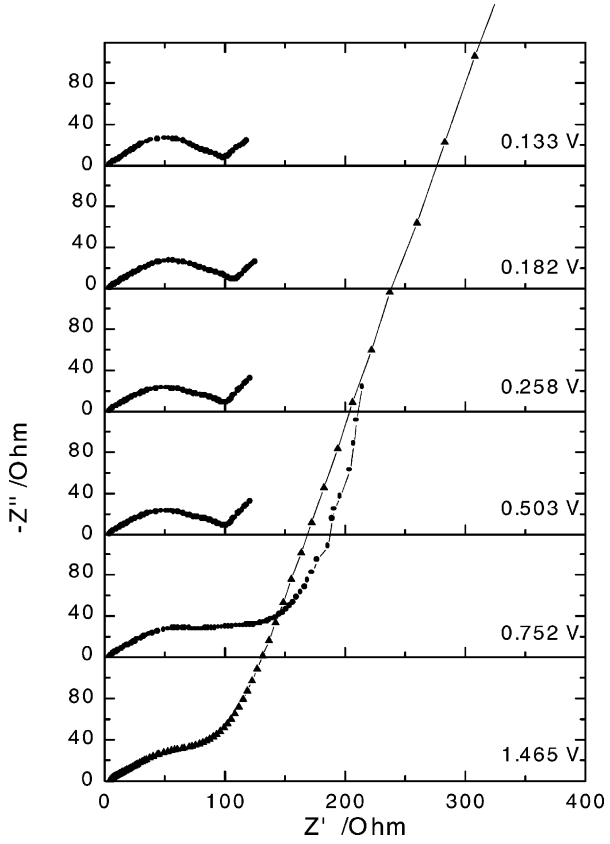

Fig. 8. Variation of impedance spectra of Li–C half-cell in 1 M $LiPF_6$ + EC/BL (1:1 v/v) during first charge (Li de-intercalation) process.

mentioned before, but that of "graphite only" results from only the carbon electrode. Finally, the low-frequency vertical lines of these two systems are all induced from the capacitive effect of carbon electrodes without lithium atoms.

When the cell is activated (lithium atoms intercalated into carbon), the impedance spectra become more complex, as shown in Fig. 11. As discussed previously, it is not possible to determine how a single electrode quantitatively contributes to the cell impedance, so the three-electrode systems with a lithium metal working electrode (labelled "lithium only") and a carbon working electrode are required for under this condition. Consider the intercept at the left side first, the R_{ex} of the "full cell" is about 7.2 Ω, that of "lithium only" is about 2.59 Ω, and that of "graphite only" is about 4.74 Ω. If the last two terms are added, the sum is 7.33 Ω, which matches the R_{ex} of the "full cell". Moreover, the spectrum of "lithium only" displays three semicircles which are the main impedance sources of "full cell". In the "lithium only" system, the reference and working electrodes are all lithium metals so that the impedance involves a passivated film, charge transfer and diffusion resistance. Owing to different electrode areas in the "lithium only" system (the reference electrode is far smaller than the working electrode), however, its spectrum is different from the Li–Li symmetric cell with the same electrode areas.

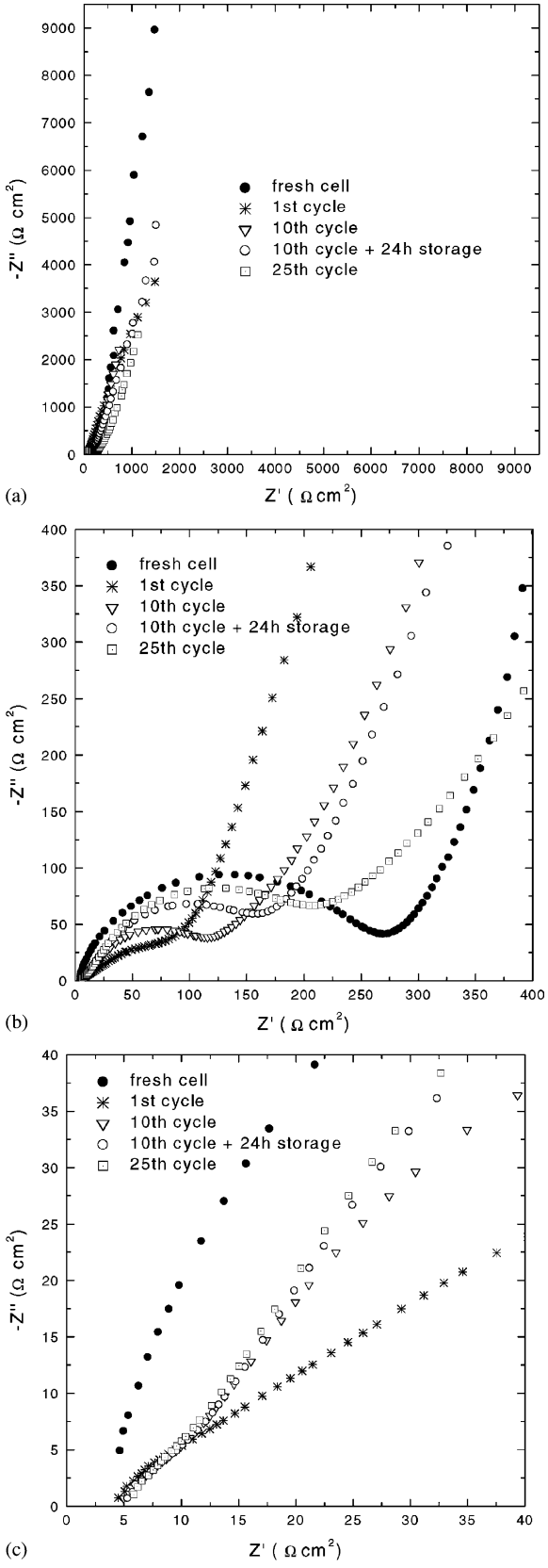

Fig. 9. Impedance spectra of Li–C half-cell in 1 M $LiPF_6$ + EC/BL (1:1 v/v) with cycling tests. (a) Spectrum in total-frequency range. (b) Enlargement in middle-high frequency range. (c) Enlargement in high-frequency range.

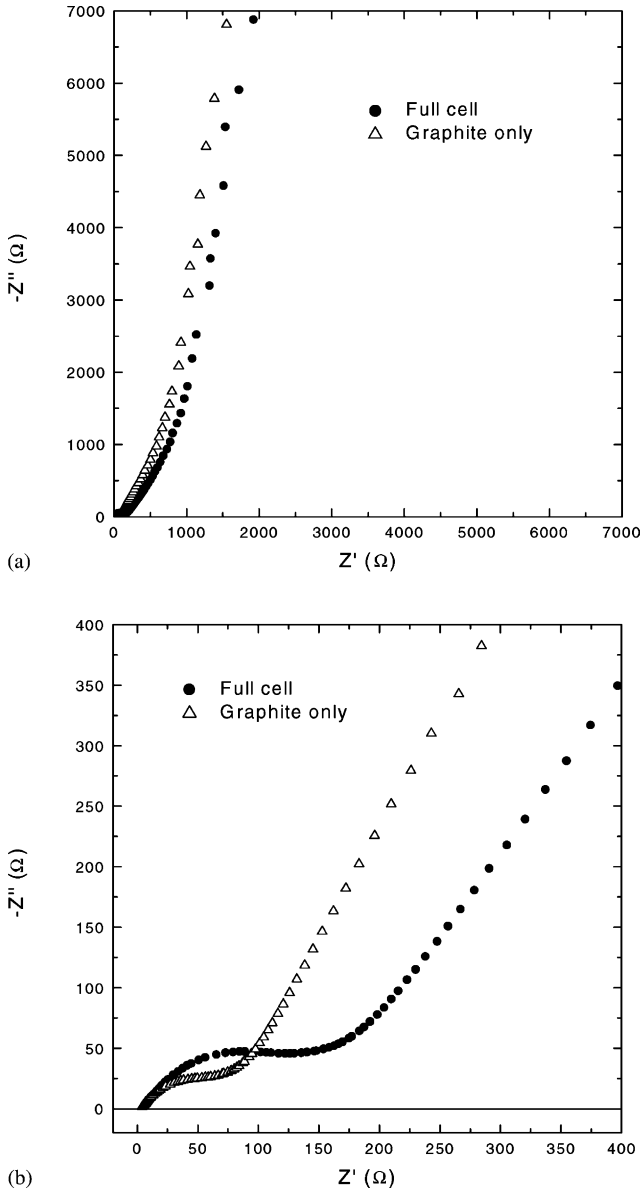

Fig. 10. Impedance spectra of Li–C half-cell measured in two- and three-electrode configurations. (a) Spectrum of total-frequency range. (b) Enlargement of high-frequency range.

It is noticeable that the "graphite only" spectrum represents two capacitive loops followed by an inductive loop. The left capacitive loop is related to the intrinsic resistance and the contact resistance of the carbon electrode, the solution resistance in carbon, and the passivated film produced by electrochemical reduction on carbon. The right capacitive loop at middle frequency corresponds to the charge-transfer resistance [12–14]. In particular, an inductive loop appears in the low-frequency region, which has been confirmed by repeated tests. This has also been reported in earlier studies [10,11]. Generally speaking, the phenomenon usually exists under conditions of rough electrodes or electrosorption of corrosion processes [15,16] fuel cells [17] and electrodeposition systems [18]. Hence, it is concluded that

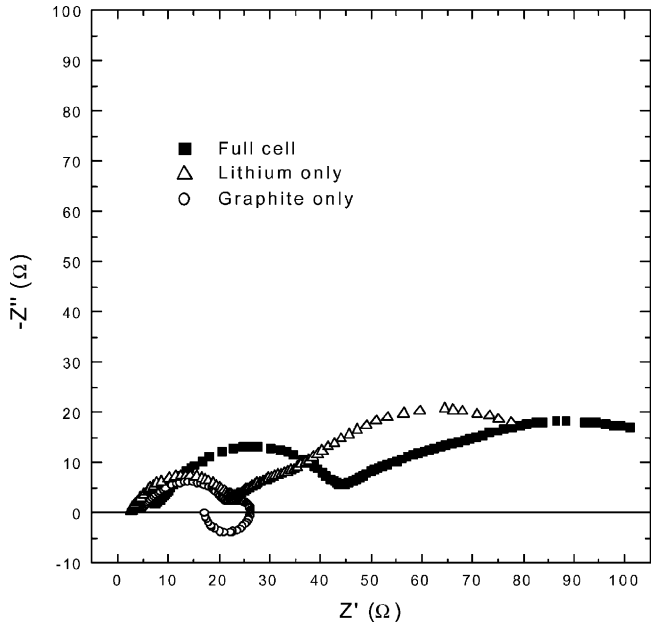

Fig. 11. Impedance spectra of Li–C half-cell after first Li intercalation into graphite measured in two- and three-electrode configurations.

this inductive loop corresponds to adsorption during lithium intercalation into carbon. This suggestion is consistent with that of Takasu et al. [19] who found that Li atoms partly undergo Farady adsorption on the carbon surface and then contribute to the capacity.

Karden et al. [10] and Nagasubramanian [11] used Li-ion batteries and lead–acid batteries and observed that the impedance spectrum of the two-electrode system is equal to the sum of the spectra of the positive and the negative electrodes in a three-electrode system. A similar approach was attempted here and it was found this addition rule also applies to Li–C half-cells as shown in Fig. 12. To prove it further, the same analysis was repeated by using the cells after 50 cycles. The results are shown in Fig. 13 and again the addition rule is confirmed. Thus, this additive property can be a criterion for impedance measurement [2].

3.3. Three-electrode impedance studies of commercial Li-ion cells

There are few reports of three-electrode impedance measurements for commercial Li-ion batteries because it is difficult to place reference electrodes inside the cells. In this study, the commercial 093488 prime Li-ion cells (1100 mAh) of SYNergy ScienTech Corp. has been used as an example for three-electrode impedance tests. The cell has stacked electrodes instead of the wound ones which are commonly used.

The two- and three-electrode impedance spectra of the 093488 Li-ion cells after the first lithium intercalation step are shown in Fig. 14. The spectra are similar to those shown in Fig. 11, except for the additional inductive effect in the

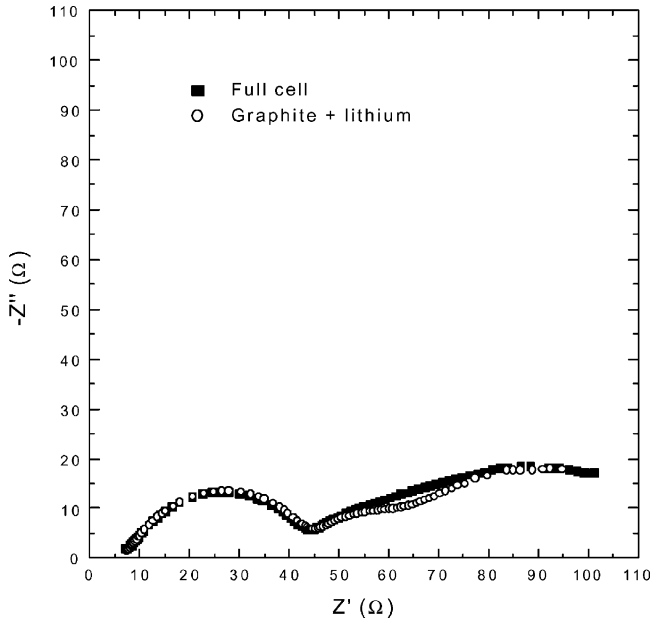

Fig. 12. Impedance spectra of Li–C half-cell after Li intercalation into carbon measured in two-electrode and sum of those of positive and negative electrodes in three-electrode configurations.

high-frequency range. The cathode is the major source of cell impedance. It is interesting that this inductive effect was not found in tests with coin cells (Figs. 2–9) or test cells (Figs. 10–13). In previous investigations, this phenomenon was observed in commercial batteries with large capacity rather than with small capacity [10,11]. Karunathilaka et al. [20] proposed that, for high-capacity cells with small inner resistance, the inductive effect results from the connecting leads of the instrument. For this reason, the two terminals of the instrument for the impedance test in the present study were connected and the spectrum of the ground impedance of the instrument was obtained, as shown in Fig. 15. The resistance of the connecting leads is up to 104 mΩ. To obtain the true impedance of cells, the ground impedance should be subtracted. The real spectra which contains no high-frequency inductive effect is shown in Fig. 16.

When the spectra of cathode and anode are added together, it is found that the combined spectra are not equal to that for the full cell, as shown in Fig. 17. This may be interpreted in terms of some simple equations as listed below. The measured impedance of a full cell is set as Z^*_{cell}, which is the sum of the real impedance of a cell (Z_{sys}) and the ground impedance of instrument (Z_{nonsys}).

$$Z^*_{\text{cell}} = Z_{\text{sys}} + Z_{\text{nonsys}} \tag{1}$$

The same situation exits in measuring the anode and cathode, i.e.

$$Z^*_{\text{anode}} = Z_{\text{anode}} + Z_{\text{nonsys}} \tag{2}$$

$$Z^*_{\text{cathode}} = Z_{\text{cathode}} + Z_{\text{nonsys}} \tag{3}$$

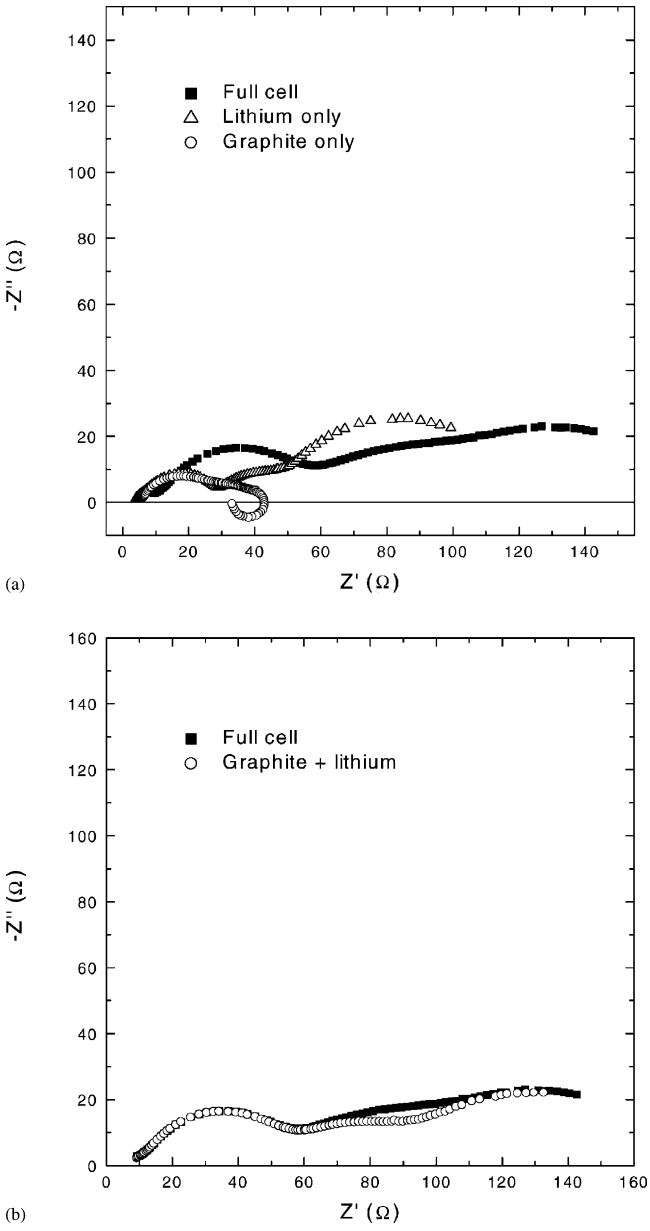

Fig. 13. Impedance spectra of Li–C half-cell after 50 cycles. (a) Spectra of two- and three-electrode configuration. (b) Spectra of two-electrode system and sum of spectra of positive and negative electrode in three-electrode system.

where Z^*_{anode} and Z^*_{cathode} are the measured impedance of the anode and the cathode; Z_{anode} and Z_{cathode} are the real impedance of the anode and the cathode.

According to the addition rule discussed above:

$$Z_{\text{sys}} = Z_{\text{anode}} + Z_{\text{cathode}} \tag{4}$$

and

$$\begin{aligned} Z_{\text{sum}} &= Z^*_{\text{anode}} + Z^*_{\text{cathode}} \\ &= (Z_{\text{anode}} + Z_{\text{nonsys}}) + (Z_{\text{cathode}} + Z_{\text{nonsys}}) \\ &= (Z_{\text{anode}} + Z_{\text{cathode}} + Z_{\text{nonsys}}) + Z_{\text{nonsys}} \\ &= (Z_{\text{sys}} + Z_{\text{nonsys}}) + Z_{\text{nonsys}} = Z^*_{\text{cell}} + Z_{\text{nonsys}} \end{aligned} \tag{5}$$

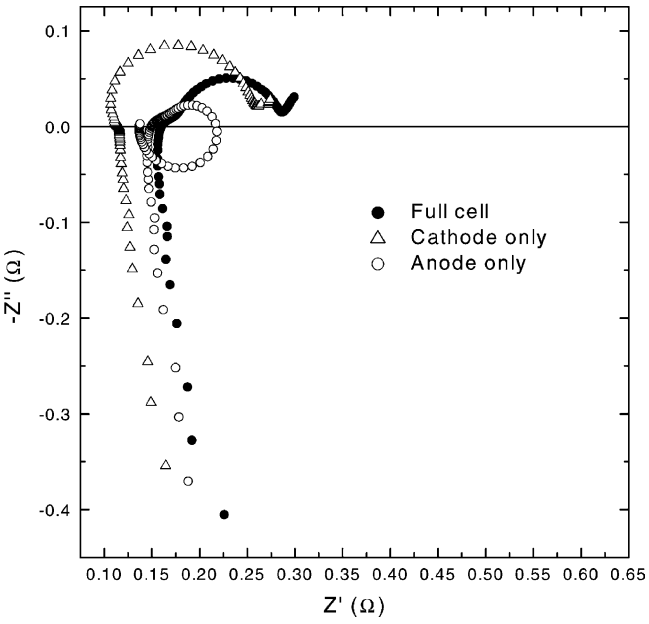

Fig. 14. Impedance spectra of 093488 prime Li-ion cell (1100 mAh) measured in two-electrode and three-electrode configuration after first Li intercalation step.

If Z_{nonsys} is small enough to be negligible, Z_{sum} is equal to Z^*_{cell}. This means the sum of the spectra of the anode and the cathode is equal to that of the full cell. This is consistent with the discussion above.

In commercial batteries, however, Z^*_{cell} and Z_{nonsys} have the same order so that Eq. (5) should be taken into account. Thus, the ground impedance shown in Fig. 15 is subtracted from the sum of the impedances of the anode and the cathode and the corrected spectrum shown in Fig. 17 was obtained. This spectrum is consistent with the spectrum for a full cell.

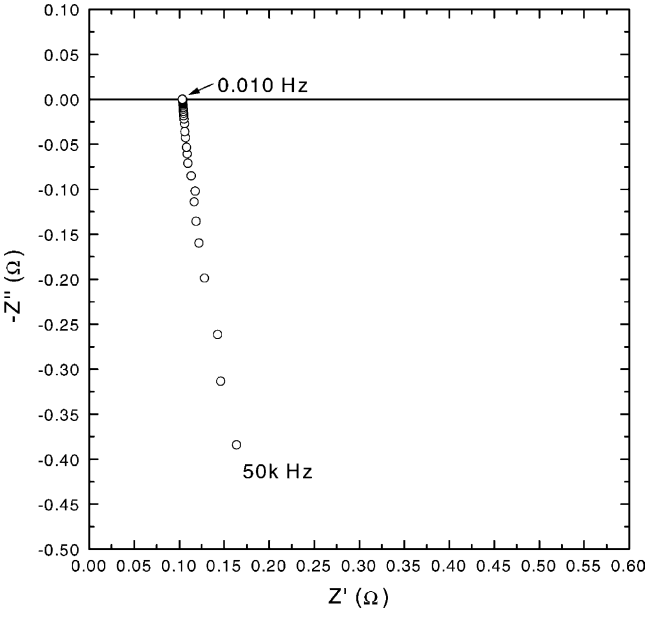

Fig. 15. Impedance spectrum of connecting leads of instrument.

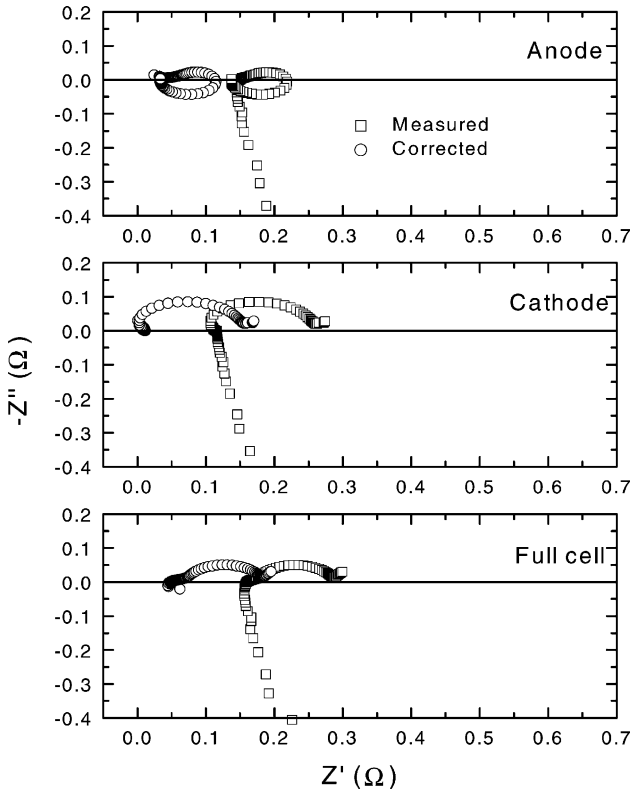

Fig. 16. Measured and corrected impedance spectra of two electrodes and full cells of 093448 prime Li-ion batteries.

To check this analysis, a cell after 100 cycles was taken as an example to repeat the same study, as shown in Fig. 18. The results provide the required confirmation.

Finally, the impedance spectra of the anode, the cathode, and the full cell with increasing cycle number are displayed

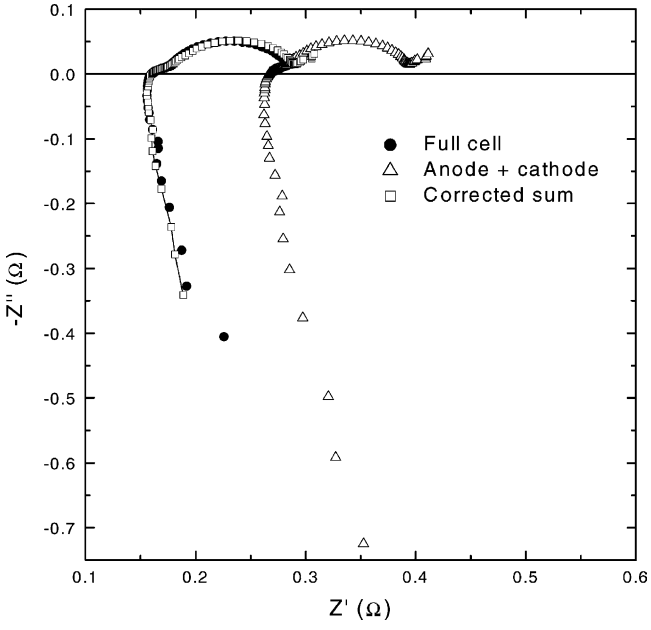

Fig. 17. Check of summation of cells in Fig. 13.

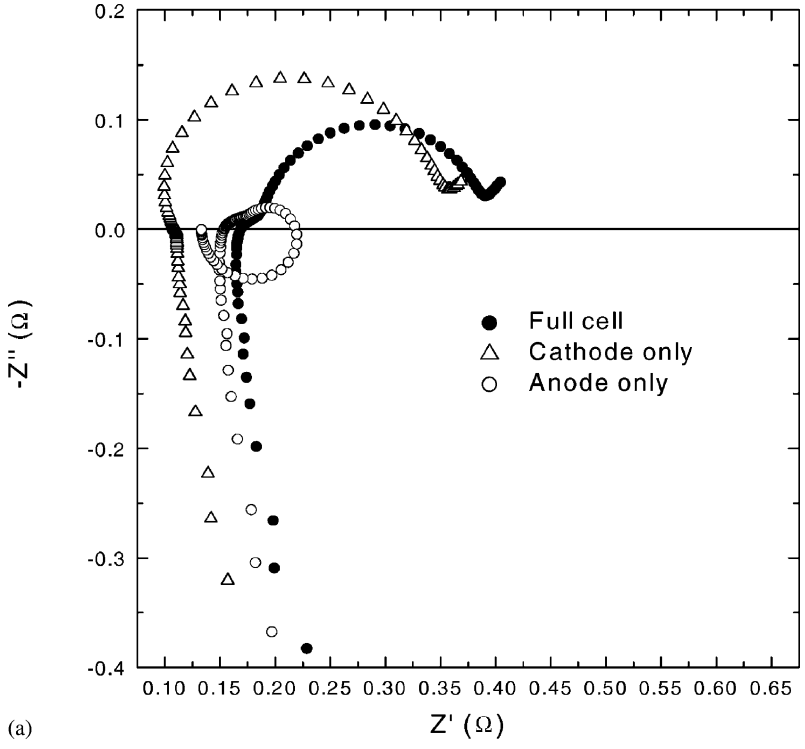

(a)

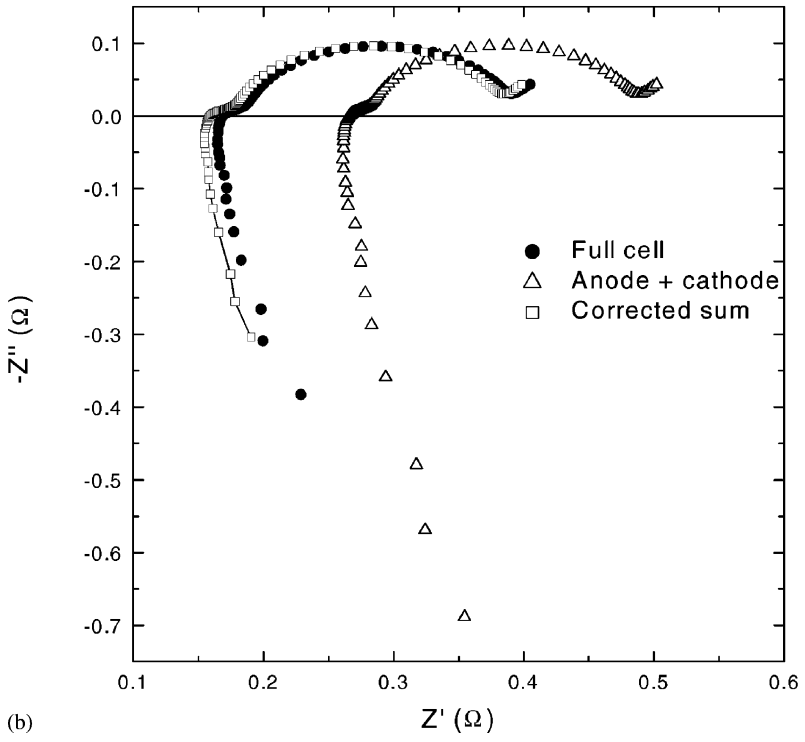

(b)

Fig. 18. Impedance spectra of 093448 prime Li-ion batteries after 100 cycles. (a) Measurement in two- and three-electrode configuration. (b) Check of summation of cells in (a).

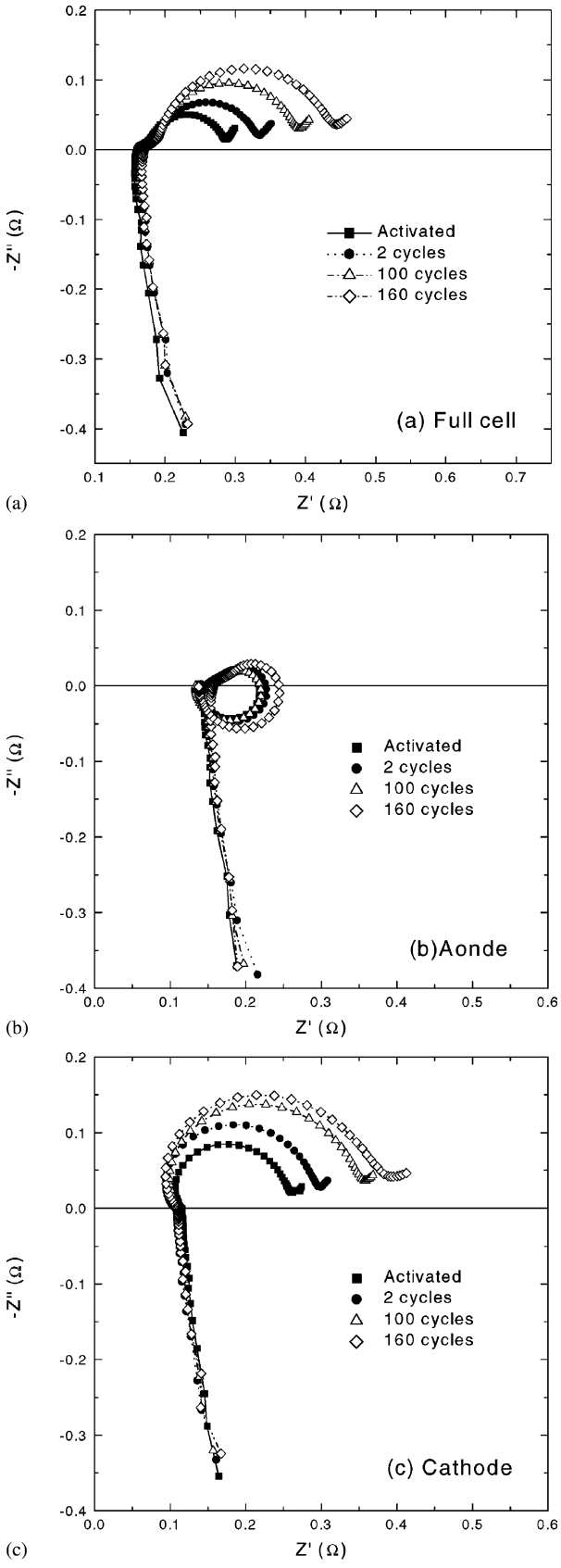

Fig. 19. Impedance spectra of 093448 prime Li-ion batteries with cycling tests: (a) full cell; (b) anode: graphite; (c) cathode: $LiCoO_2$.

in Fig. 19. For the full cell, the capacitive loop at high frequency retains its shape, but the one at middle–low frequency continually rises. After 160 cycles, the resistance of the fresh cell doubles. Judging from the charging property of the cathode impedance and the anode impedance in Fig. 19, it is obvious the major source of cell impedance comes from the cathode.

4. Conclusions

In this study, the results of systematic and integrated comparisons of two- and three-electrode electrochemical impedance measurements are presented. From analysing and comparing these spectra, the real physical meaning and the variation of impedance during cycling are evaluated. Consequently, several key points related to the application of impedance spectroscopy to Li-ion batteries can be pointed out as follows:

1. In the two-electrode study, preliminary study of a symmetric half-cell must be carried out for reference data. Information on the single electrode can then be obtained.
2. An inductive loop appears in the low-frequency region of the spectrum of a carbon electrode and decreases after the first lithium-intercalation step. This probably implies that an adsorption–desorption phenomenon exists at the interface.
3. For batteries with small interior resistances, an inductive effect arising from the connecting leads would appear in the high-frequency region. This ground resistance needs to be deducted from the impedance spectra so that correct interpretation can be made.
4. The impedance spectrum of the two-electrode system is equal to the sum of the spectra of the positive and the negative electrodes in a three-electrode system.
5. The major source of cell impedance comes from the positive electrode (cathode) in a lithium-ion battery.

References

[1] A. Funabiki, M. Inaba, Z. Ogumi, S.-I. Yuasa, J. Otsuji, A. Tasaka, J. Electrochem. Soc. 145 (1998) 172.
[2] D. Aurbach, B. Markovsky, M.D. Levi, E. Levi, A. Schechter, M. Moshkovich, Y. Cohen, J Power Sources 81/82 (1999) 95.
[3] C.R. Yang, J.Y. Song, Y.Y. Wang, C.C. Wan, J. Appl. Electrochem. 30 (2000) 29.
[4] B. Markovsky, M.D. Levi, D. Aurbach, Electrochim. Acta 43 (1998) 2287.
[5] D. Aurbach, B. Markovsky, I. Weissman, E. Levi, Y. Ein-Eli, Electrochim. Acta 45 (1999) 67.
[6] Y.C. Chang, H.J. Sohn, J. Electrochem. Soc. 147 (2000) 50.
[7] M. Dollé, F. Orsini, A.S. Gozdz, J.M. Tarascon, J. Electrochem. Soc. 148 (2001) A851–A857.
[8] M. Gaberšèek, S. Pejovnik, J. Electrochem. Soc. 146 (1999) 933–940.

[9] M. Gaberšèek, J. Jamnik, S. Pejovnik, J. Electrochem. Soc. 140 (1993) 308–315.
[10] E. Karden, S. Buller, R.W. De Doncker, J. Power Sources 85 (2000) 72.
[11] G. Nagasubramanian, J. Power Sources 87 (2000) 226.
[12] A. Funabiki, M. Inaba, Z. Ogumi, S.I. Yuasa, J. Otsuji, A. Tasaka, J. Electrochem. Soc. 145 (1998) 172.
[13] E. Barsoukov, J.H. Kim, J.H. Kim, C.O. Yoon, H. Lee, J. Electrochem. Soc. 145 (1998) 2711.
[14] Y.C. Chang, H.J. Sohn, J. Electrochem. Soc. 147 (2000) 50–58.
[15] N.A. Hampson, S.A.G.R. Karunathilaka, R. Leek, J. Appl. Electrochem. 10 (1980) 3–11.
[16] D.A. Harrington, B.E. Conway, Electrochim. Acta 32 (1987) 1703–1712.
[17] J.T. Müller, P.M. Urban, W.F. Hölderich, J. Power Sources 84 (1999) 157–160.
[18] R. Wiart, Electrochim. Acta 35 (1990) 1587–1593.
[19] R. Takasu, K. Sekine, T. Takamura, J. Power Sources 81/82 (1999) 224–228.
[20] S.A.G.R. Karunathilaka, R. Barton, M. Hughes, N.A. Hampson, J. Appl. Electrochem. 15 (1985) 251–257.